Construction and Building Materials 220 (2019) 456–463

Contents lists available at ScienceDirect

Construction and Building Materials

journal homepage: www.elsevier.com/locate/conbuildmat

Stress-strain relationship of cement mortar under triaxial compression

Mithaq Kohees [a,b], Jay Sanjayan [a], Pathmanathan Rajeev [a,*]

[a] Department of Civil and Construction Engineering, Swinburne University of Technology, Hawthorn, Victoria 3122, Australia
[b] Civil Engineering Department, College of Engineering, Al-Mustansiriyah University, Baghdad, Iraq

HIGHLIGHTS

- New stress-strain model for cement mortar under triaxial stress state is presented.
- The stress-strain model parameters are developed using the experimental data.
- The developed model can be used to analytically or numerically predict the performance of cement mortar subjected to the various stress states.

ARTICLE INFO

Article history:
Received 10 July 2018
Received in revised form 17 May 2019
Accepted 23 May 2019
Available online 11 June 2019

Keywords:
Mortar
Constitutive model
Confining pressure
Volume change
Ductility

ABSTRACT

This paper presents a study on the stress-strain relationship of cement mortar under triaxial stress state. The influence of confining pressure on peak-stress, peak-strain, volume change, modulus of elasticity, and Poisson's ratio were studied using experimental results and data from limited studies in the literature. Cement mortar samples having compressive strengths of 38 MPa and 45 MPa were tested under four levels of confining pressures (i.e., 0, 5, 10, and 15 MPa) and a stress-strain model for confined cement mortar was subsequently developed. It has been shown that the model has good agreement with both the experimental results. The results not only show that confinement significantly improves the strength and ductility of the cement mortar samples, but also reveal a linear relationship between the observed lateral and axial strain. In this regard, the mathematical relationship for confined cement mortar was developed as a function of the stress and strain parameters of the unconfined state and a new linear relationship between modulus of elasticity, Poisson's ratio and lateral stress is proposed.

1. Introduction

Cement mortar materials are widely used in normal construction, mining and 3D concrete printing applications [1,2]. In order to design and safety assessment of structures, the mechanical properties under complex stress conditions due external loadings are required. For cement mortar made of same materials, the mechanical properties are different when the material mixture ratio is different, and the mechanical properties of the specimens are also different when the loading is different [3].

Hence the accurate prediction of stress-strain behaviour of cement mortar under various stress state is required to be developed for the accurate estimate of the structural performance. Specifically, considering the performance of mortar under triaxial compression and/or tension is useful for masonry structures for the determination of strength, deformation and failure modes.

A comprehensive review of past literature on the mechanical behaviour of unconfined and confined cement mortar reveals that limited models are available to describe partially the mechanical behaviour of cement mortar. However, none of these models develop the complete stress-strain behaviour of cement mortar under triaxial stress states. For example, the brickwork failure criteria under multiaxial stress conditions was studied by Khoo [4] through the effects of lateral stress on the modulus of elasticity and Poisson's ratio of cement mortar considering two different mix designs (i.e., 1:0.25:3 and 1:1:6 with w/c ratio of 0.64 and 1.29 respectively) and concluded that a linear model is best at describing the relation between peak axial stress and confinement ratio (failure envelope) of cement mortar. Also, it was observed that the magnitude of the initial modulus of elasticity increases with the increase of lateral stress, whereas the Poisson's ratio decreases. McNary et al. [5] considered cylindrical specimens of four different mixes under confinement and reported that the decrease of lateral strain as well as Poisson's ratio and the increase of modulus of elasticity. Moreover, the relation between ultimate axial stress and lateral confinement can be represent by a linear equation. The studies by Atkinson et al. [6] and Mohamad [7] further confirmed the findings of Khoo and McNary. Hayen et al. [8] studied the triaxial mechanical interaction of four different

* Corresponding author.
E-mail address: prajeev@swin.edu.au (P. Rajeev).

https://doi.org/10.1016/j.conbuildmat.2019.05.146
0950-0618/

mortar when used alongside masonry of brick and/or natural stones (the stress state of specific mortar joints under triaxial compression) to improve existing models used for determining the mechanical behaviour of historical masonry structures. The study has identified that under triaxial compression, two types of failure can occur in a mortar joint when the relationship between lateral and vertical stresses (k) < 0.25, shear mechanisms failure appear due to decrease followed by increase in volume. However, when $k \geq 0.25$ the pore collapse will occur due to change in failure mechanism to a linear decrease in volume. Barbosa et al. [9] in 2007, examined the analysis of mechanical behaviour of bedding mortar samples under triaxial compression tests. Of the three different mortar mixes used, two were casted into specimens that were demoulded after a day and kept exposed to laboratory conditions for testing, whereas the other was casted into gypsum moulds to assist in determining the effects of water-loss that occurs in bedding joints. Nevertheless, all mixes were tested under triaxial compression with confining pressures of 0, 1.5, 3, and 4.5 MPa. They concluded that it was probable to display results about mortar behaviour under triaxial effect carried out by individual researchers with different mortar mixes and varied confining stages. It was further observed that with the increase of lateral stress, the ultimate longitudinal strain had increased, and the lateral strain had decreased. Furthermore, all failure envelops could be represented by a linear function and the relationship between peak compressive strength and lateral stress could be well approximated by an equation of the 2nd order. Mohamad et al. [10], considered the triaxial test of cement mortar sample under confinement, and examined the triaxial test results on compressive strength, modulus of elasticity, and Poisson's ratio. It was reported that the researched work agreed well with the outcomes of previous studies [4,5]. In 2016, the influence of high confinement pressure (up to 300 MPa) on cement mortar was experimented by Karinski et al. [11]. Fine aggregate and w/c ratio effects on suggested model (state equation) was also investigated. It was obtained that the improvement of an experimental setup in order to apply a high lateral pressure on cement mortar is possible to achieve. Moreover, based on the multi scale approach, a new theoretical equation of state was introduced. The suggested formula was exhibited for dry materials only that gives good agreement with the obtained test results

It is therefore evident that despite the limited research regarding the behavior of cement mortar under triaxial stress as presented above, a study of the complete stress-strain constitutive model for cement mortar under lateral confinement does not exist. Therefore, this paper attempts to address this deficiency and presents a new constitutive model for cement mortar to determine the complete stress-strain behavior when under constant lateral pressure. The proposed model has been justified against experimental results obtained through the testing of several cement mortar specimens under varying confinement stresses (0–15 MPa) and reported experimental data from past research works.

2. Experimental program

2.1. Materials and specimen preparation

Two types of cement mortar samples were prepared from Geelong cement (Type GP) conforming to AS3972, and river sand with particle size distribution shown in Fig. 1. The particle density in saturated surface dry condition (SSD) of 2620 kg/m^3, moisture absorption of 0.3%, respectively.

The samples with cement to sand ratio of 1:2 and 1:3 and water to cement ratio of 0.4 and 0.6 were considered in this study. The samples were prepared using a mechanical mixer which was operated at 80 rpm in accordance with ASTM C305-14 [12]. Altogether 18 specimens were casted, where each mixture had six that were cylindrical with a 38 mm diameter and 76 mm height and three that were cubic with 50 mm sides for compression tests. All specimens were compacted and vibrated in layers, where on completion were covered with plastic sheets to prevent water-loss and were kept at laboratory conditions for a day prior to demolding and immersing into water of 23 °C for 28 days. Table 1 provide the mix details and uniaxial compressive strength. Fig. 2 shows the stress-strain curves under uniaxial stress for each mix.

2.2. Experimental setup

Fig. 3 shows the setup of the triaxial system. The average axial strain was measured between spring-loaded rings that would be

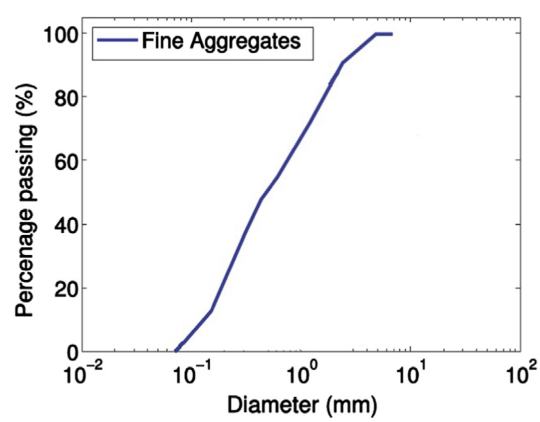

Fig. 1. Fine aggregate grain size distribution.

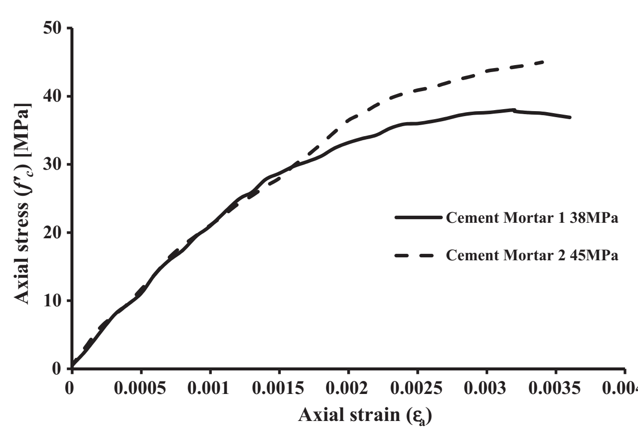

Fig. 2. The axial stress-strain curves of both mortar mixes.

Table 1
Base material composition of each mix.

Mortar Mix	W/C Ratio	Cement (g)	Sand (g)	Water (g)	Triaxial Test Specimens	Comp. Test Specimens	Comp. Strength (MPa)
1	0.6	1000	3000	600	6	3	38
2	0.4	1000	2000	400	6	3	45

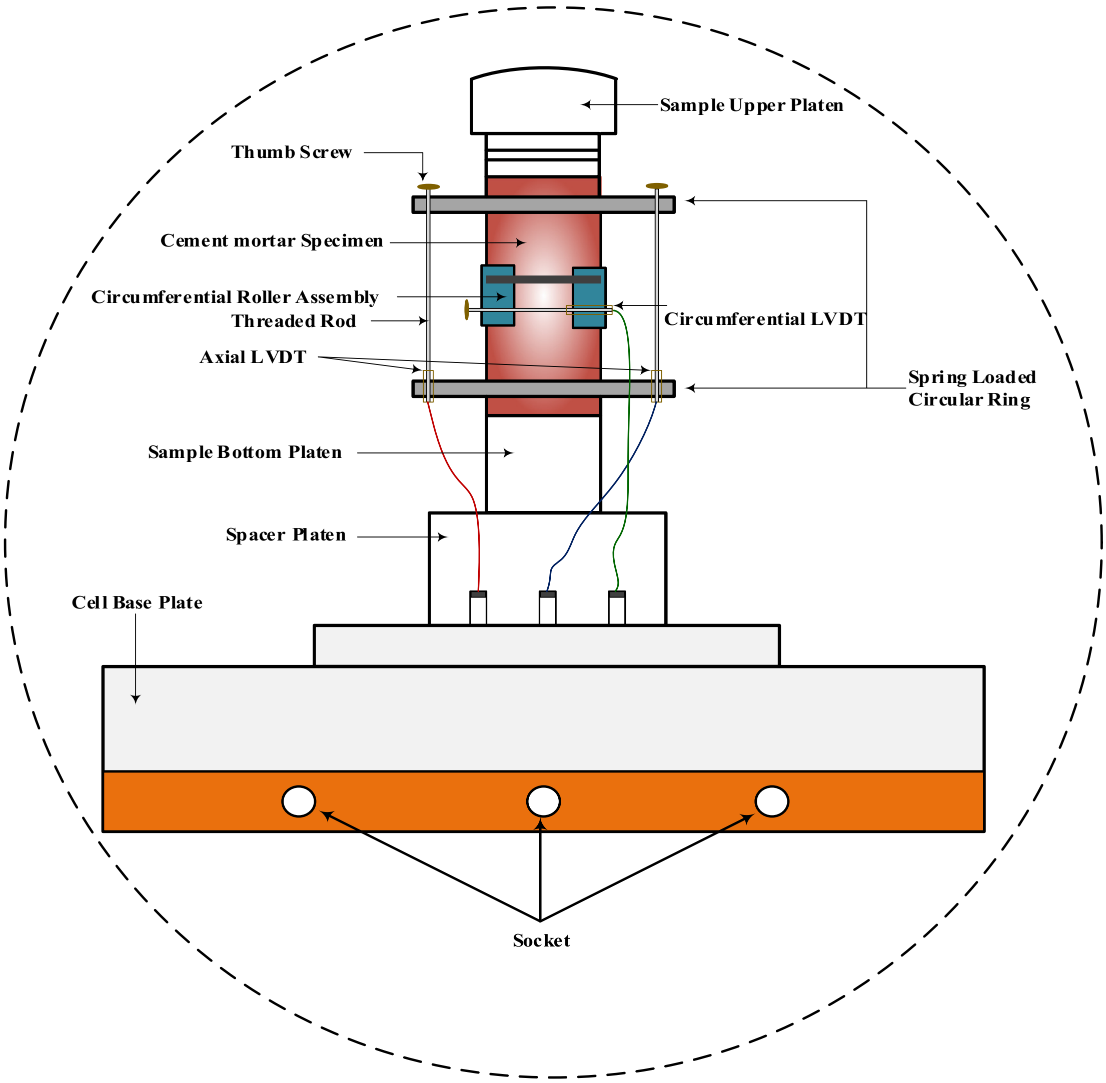

Fig. 3. The schematic representation of the triaxial system.

mounted on the specimen and via two axial LVDTs, whereas a circumferential LVDT at mid-height was used to measure circumferential strain. A universal testing machine, with 1 MN capacity, was used for applying axial stress at an axial displacement rate of 0.2 mm per minute on grounded and prepared specimens under a variety of constant confining pressures (0, 5, 10, and 15 MPa) that were applied by pressurised fluid via a regulated air driven piston, where the required air pressures ranged between 100 and 700 kPa (1–7 bars). The required date was acquired using a SCON-1500 universal signal conditioning and control unit.

3. Experimental results

3.1. The behaviour of axial strain at peak compressive strength

Many researchers have indicated that the axial strain at peak compressive stress is an essential parameter for developing a stress-strain relationship when under triaxial compression. Such studies, for a variety of material specimens, have shown that axial strain was dependent on parameters such as compressive strength [13–18] or both compressive strength and modulus of elasticity [19,20], where the functional relationship would either be linear or based on a power law. This study, on the other hand, proposes a simplified linear relationship as expressed in Eq. (1) for the behaviour of axial strain (in units of $\mu\varepsilon$) at peak compressive strength (in units of MPa) and was established using experimental test results as well as data reported in the literature [7,8,9,21,22] as shown in Fig. 4. The proposed Eq. (1) has good agreement with experimental results and has a similar trend as that of concrete, whereas compressive strength of the cement mortar increases, axial strain at peak compressive stress also increases.

$$\varepsilon_{ac} = 80(f'_c) \quad (1)$$

where ε_{ac} = axial strain at unconfined axial stress, and f'_c = maximum unconfined stress in MPa.

3.2. The behaviour of modulus of elasticity and Poisson's ratio under confinement

The effect of lateral stress on the modulus of elasticity and Poisson's ratio for cement mortar under triaxial compression is investigated in this part of the study and compared with both experimental results and data available in literature. Experimental results have established that lateral pressure will affect the behaviour of cement mortar, and the influence of confining pressure on the initial modulus of elasticity as well as the initial Poisson's

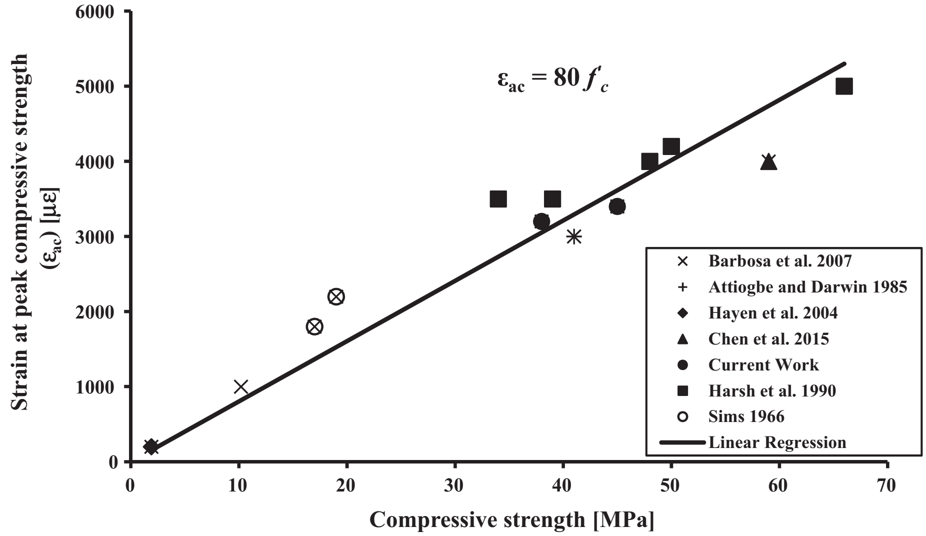

Fig. 4. Axial strain at peak compressive strength for cement mortar.

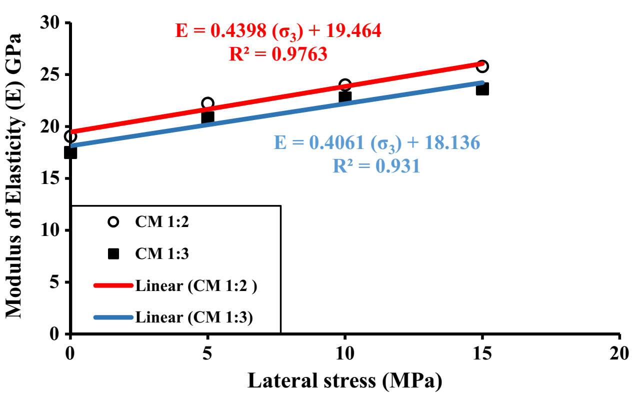

Fig. 5. The behaviour of modulus of elasticity under lateral confinement.

ratio is evident as shown in Fig. 5. Though it is seen that the initial values for the modulus of elasticity increases with the increase of lateral stress, those of the initial Poisson's ratio decrease. This behaviour is observed in other studies as well [4,5,6,7,10]. Furthermore, a linear relationship is proposed for the behaviour of the ratio between modulus of elasticity and the maximum unconfined axial stress against the confinement ratio, and for the behaviour of Poisson's ratio against confinement ratio (Eqs. (2) and (3), respectively, where confined ratio is defined as the ratio between applied lateral stress and maximum unconfined axial stress). This is depicted in Figs. 6 and 7 respectively as well.

$$\frac{E}{f'_c} = 112.51\frac{\sigma_3}{f'_c} + 635.85 \quad (2)$$

$$\nu = -0.0895\frac{\sigma_3}{f'_c} + 0.1374; \ \frac{\sigma_3}{f'_c} \leq 1.5 \quad (3)$$

where: E = Modulus of elasticity, ν = Poisson's ratio, σ_3 = confining pressure/lateral stress in MPa, and $\frac{\sigma_3}{f'_c}$ = confinement ratio.

Table 2 summarises some of the important parameters measured for each mortar mix under unconfined and confined conditions through uniaxial and triaxial testing. These were crucial for model development.

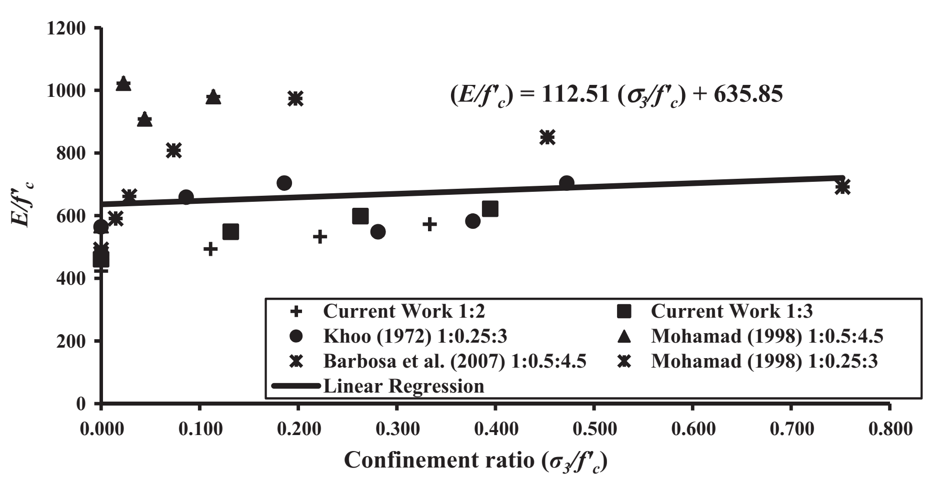

Fig. 6. Comparison of the ratio between modulus of elasticity and maximum unconfined axial stress versus lateral confinement for cement mortar.

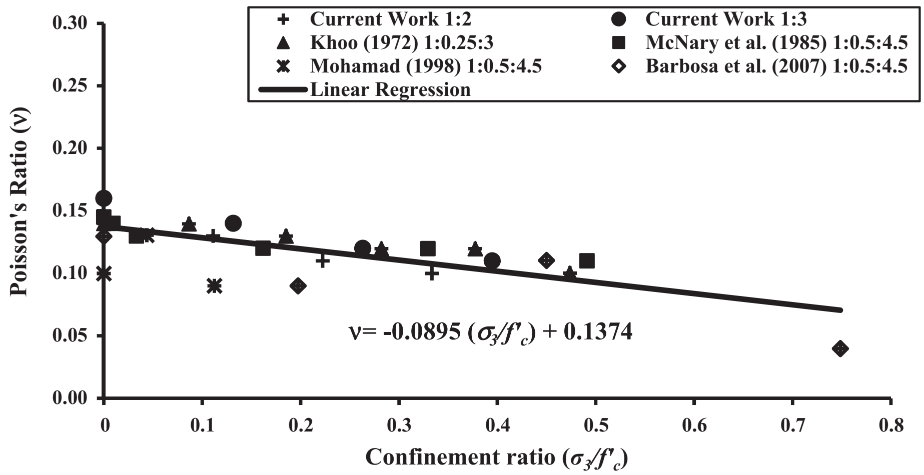

Fig. 7. Comparison of the Poisson's ratio versus confinement ratio for cement mortar.

Table 2
Summary of key parameters for each mortar mix.

Mortar Mix	Test	Confining Pressure σ_3 (MPa)	Axial Strength σ_{1c} (MPa)	Peak Lateral Strain ε_{3c}	Peak Axial Strain ε_{1c}
1	Uniaxial	0	38	−0.0016	0.0032
	Triaxial-1	5	60	−0.0029	0.0065
	Triaxial-2	10	80	−0.0038	0.0095
	Triaxial-3	15	105	−0.0046	0.0130
2	Uniaxial	0	45	−0.0017	0.0034
	Triaxial-1	5	80	−0.0039	0.0086
	Triaxial-2	10	100	−0.0046	0.0115
	Triaxial-3	15	126	−0.0056	0.0159

3.3. Peak axial stress under various confining pressures

Richart et al. [23] proposed a linear relationship between peak axial stress and the level of confinement as shown in Eq. (4). This equation depends on the coefficient (k) as per the general Mohr-Coulomb failure criterion, which helps to identify the ultimate axial stress at a certain level of confinement for any constitutive model of cement and/or concrete and can yield significantly large values for peak axial stress as confinement pressure is increased.

$$\frac{\sigma_1}{f_c'} = 1 + k\left(\frac{\sigma_3}{f_c'}\right) \quad (4)$$

where: σ_1 = peak axial stress in MPa, and k = confinement coefficient.

Commonly, for concrete, the values for the coefficient, k, range between 4 and 6. However, through this study, it was found to be 4.9 through linear regression and is as shown in Fig. 8. Khoo [4] specified a value of k equal to 3.4 for uniaxial strength of 24 MPa, Atkinson et al. [6] reported a value of 5 for the coefficient k, for cement mortar of 32.6 MPa compressive strength. While, Mohamad [7] indicated a k value of 4 for unconfined compressive strength of 23 MPa. Considere [24] reported a value of 4.8 for the coefficient k from triaxial tests on mortar cylinders of 300 mm in diameter and 800 mm in height with compressive strengths of 5.2, 7.3, 9, and 16.7 MPa and lateral confinements of 0, 2, 5, 10, and 15 MPa. Balmer [25] reported an average value of 5.6 for the coefficient k from triaxial tests on concrete cylinders of 150 mm in diameter and 300 mm in height having a compressive strength of 25 MPa under confining pressures varying from 0 to 172.4 MPa (until failure). Moreover, Nielsen [26] published the values of 3 and 8 for the coefficient k from triaxial tests with active confinement on specimens made of two different steel fibre reinforced ultra-high strength mortar mixes that were of 100 mm in diameter and 200 mm in height and of 165 MPa compressive strength.

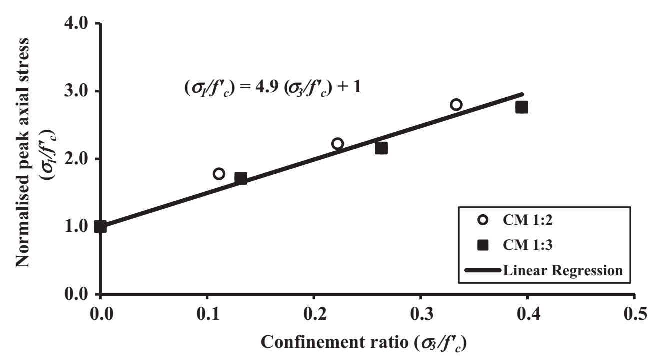

Fig. 8. Establishing the coefficient k through experimental results.

3.4. Axial strain at peak axial stress

The relationship between normalised axial strain at peak axial stress and confinement ratio is as expressed in Eq. (5) and shown in Fig. 9 and demonstrates a linear relationship. This study establishes a material parameter of 9.1.

$$\frac{\varepsilon_{au}}{\varepsilon_a} = 9.1\left(\frac{\sigma_3}{f_c'}\right) + 1 \quad (5)$$

where: ε_{au} = strain at peak axial stress in microstrain ($\mu\varepsilon$), and ε_a = axial strain.

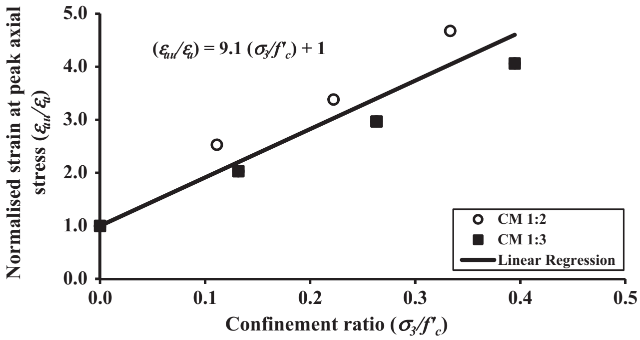

Fig. 9. Establishing the material parameter through experimental results.

3.5. Proposed model

Many studies have developed a relationship between stress and strain under different stress states for cement paste, OPC concrete, and geopolymer paste. However, only a few limited studies exist on the stress-strain behaviour of cement mortar under constant confinement (active confinement), therefore a constitutive model is required. Collins and Mitchell [20] have improved Popovics [13] model for confined stress-strain in concrete as expressed in Eq. (6). This model was found to be suitable for cement mortar and was used in this study.

$$\frac{\sigma_1}{f'_c} = \frac{n(\varepsilon_a/\varepsilon_{au})}{n-1+(\varepsilon_a/\varepsilon_{au})^{nk}} \quad (6)$$

where: σ_1 = the compressive stress of confined concrete; f'_c = maximum compressive stress of unconfined concrete; ε_a = the axial strain of concrete; ε_{au} = maximum strain at maximum stress of confined concrete; n = curve fitting factor; k = 1 when $\varepsilon_a/\varepsilon_{au} \le 1$, $k = 0.67 + f'_c/62$ when $\varepsilon_a/\varepsilon_{au} > 1$, $n = 0.8 + f'_c/17$.

The selected model was made suitable after adjusting the values of k and n in accordance with experimental results and is expressed below:

$$\frac{n^{0.25}}{\sqrt{f'_c}} = -0.0003\sigma_1 + 0.2073 \quad (7)$$

$$\frac{k}{\sqrt{f'_c}} = 0.0135\frac{\sigma_1}{f'_c} + 0.1509 \quad (8)$$

where: σ_1 and f'_c are in MPa.

Figs. 10 and 11 show the comparison between the experimental stress-strain relationship and that determined by the proposed model for mortar mixes 1 and 2 respectively.

3.6. Lateral strain at peak stress

In this study, the relationship between lateral and axial strain for cement mortar can be expressed through a linear formula that is relatable to any level of confinement as expressed in Eq. (9), though parabolic relationships have been proposed for concrete [27].

$$\varepsilon_l = \alpha(\varepsilon_a/\varepsilon_{au}) \quad (9)$$

where: ε_l = lateral strain, and α = lateral dilatation coefficient.

A linear relationship is applicable when considering the plot of the lateral dilatation coefficient against confinement ratio for both mortar mixes as shown in Fig. 12 and an increasing trend is observed. This relationship is expressed in Eq. (10).

$$\alpha = 0.0053\left(\frac{\sigma_3}{f'_c}\right) + 0.0012 \quad (10)$$

Furthermore, combining from Eq. (9) and the initial Poisson's ratio (ν_o), an expression to determine the secant Poisson's ratio can be derived as expressed in Eq. (11).

$$\nu_s = \nu_o + \frac{\alpha}{\varepsilon_{au}} \quad (11)$$

where: ν_s = secant Poisson ratio, and ν_o = initial Poisson ratio.

3.7. Volumetric dilatation and contraction

A simplified formula developed by Lokuge et al. [28] was adopted in this study to evaluate volumetric behaviour. This formula depends on the relationship between the normalised volumetric strain factor ($\bar{\varepsilon}_v$) and the normalised axial strain factor ($\bar{\varepsilon}_a$).

The normalised volumetric strain factor is defined as the ratio between volumetric strain (ε_v) and the maximum value of volumetric strain (ε_{vmax}) as expressed in Eq. (12), whereas the

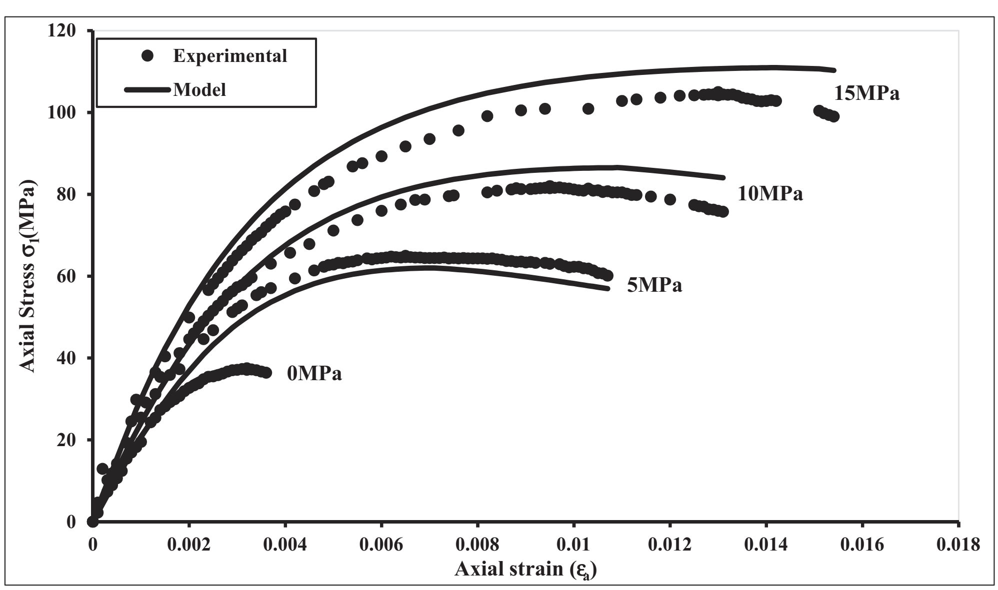

Fig. 10. Comparison of experimental and model stress-strain relationships of mortar mix 1.

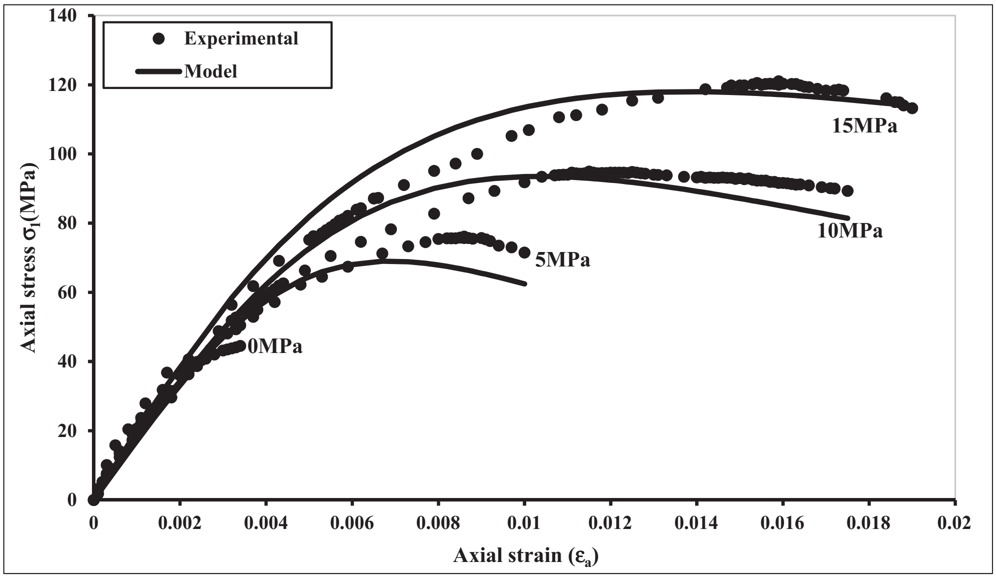

Fig. 11. Comparison of experimental and model stress-strain relationships of mortar mix 2.

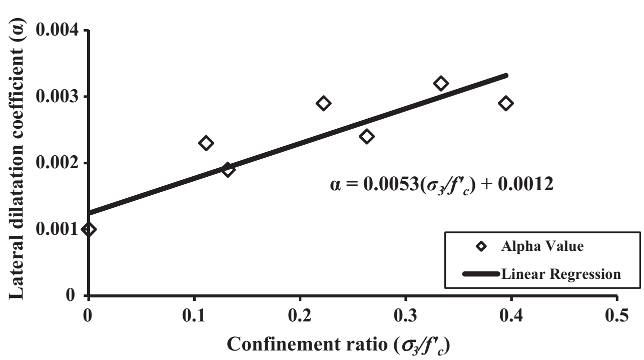

Fig. 12. Establishing a relationship between the lateral dilatation coefficient and confinement ratio considering both mortar mixes.

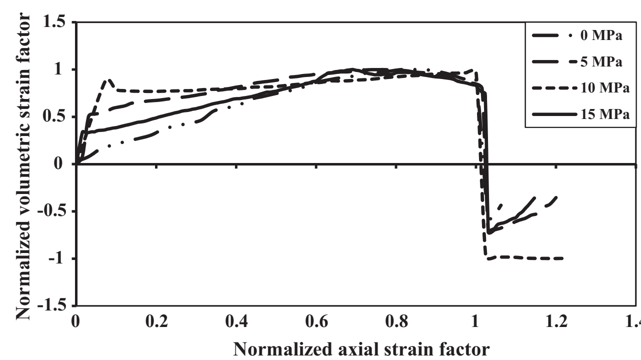

Fig. 13. Normalized volumetric strain factor vs. normalized axial strain factor for mortar mix 1.

normalised axial strain factor is defined as the ratio between axial strain (ε_a) and the axial strain at peak axial stress (ε_{au}) as expressed in Eq. (13).

$$\bar{\varepsilon}_v = \frac{\varepsilon_v}{\varepsilon_{v\max}} \tag{12}$$

$$\bar{\varepsilon}_a = \frac{\varepsilon_a}{\varepsilon_{au}} \tag{13}$$

In the current study, and by considering the research work that was done for concrete [28], it seems that the behaviour of cement mortar is almost equivalent, where volumetric strain gradually increases with increasing axial stress (contracts) until a peak value is reached. Having reached a maximum, a rapid reduction (expands) is observable and this behaviour differs from that generally observed in related studies using concrete. Within this region and in a specific point, the behaviour changes from contraction to expansion. In this study and at this particular point, the volumetric strain reaches its maximum value that's correspond to an axial strain of approximately 0.82ε_{au} for mortar mix 1, and 0.86ε_{au} for mortar mix 2, as established through Figs. 13 and 14. Moreover, It can be noticed that the volumetric strain became a zero in specific point (i.e. the sample returns to its original volume) named as the zero-volume point, this phenomenon occurs when the axial stress reaches its ultimate value, at that point volumetric strain will be equal to:

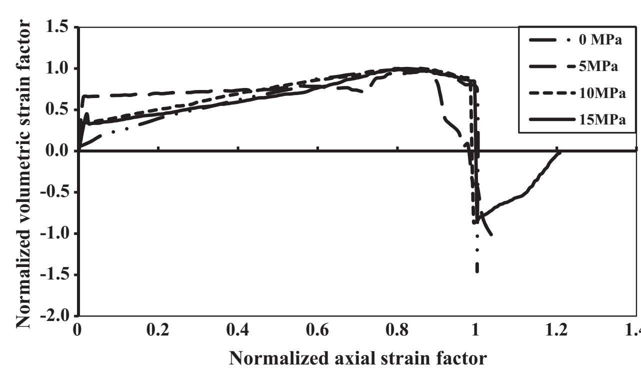

Fig. 14. Normalized volumetric strain factor vs. normalized axial strain factor for mortar mix 2.

$$\bar{\varepsilon}_v = \frac{\varepsilon_a + 2\varepsilon_l}{\varepsilon_{v,max}} = 0 \tag{14}$$

therefore,

$$\varepsilon_a = 2\varepsilon_l \tag{15}$$

It was noted that from Eq. (15), the confinement ratio seems to have no effect on the secant strain ratio at failure for the mortar mixes and when at peak stress, the secant value of the Poisson's ratio is equal to 0.5. This phenomenon is reported in other studies [28–30].

4. Summary and conclusions

The stress-strain behaviour of cement mortar under lateral confinement was investigated in this study. Two cement mortar mixes having compressive strengths of 38 and 45 MPa were subjected to triaxial tests under active confinement pressures of 0, 5, 10, and 15 MPa. The results were used to develop a complete stress-strain model for cement mortar subjected triaxial compression. The proposed model shows good agreement with experimental results. The equation for strain at peak compressive strength shows a linear relationship as observed for normal concrete, and agrees well with experimental results and data available in literature. With the increase of lateral stress, the initial value of modulus of elasticity increases and Poisson's ratio decreases. Also, a liner variation for elasticity and Poisson's ratio with confinement ratio was found for cement mortar. The developed stress-strain model can be used to predict the behaviour of cement mortar analytically or can be implemented in numerical programmes.

Declaration of Competing Interest

There is no conflict of interest.

Acknowledgements

The first author acknowledges the Republic of Iraq, Ministry of Higher Education and Scientific Research for the Postgraduate research award. The authors also acknowledge the assistance of the Smart Structures Laboratory staff of Swinburne University of Technology during the experimental work of the research reported in this paper.

References

[1] X.S. Liu, Q.H. Gu, Y.L. Tan, J.G. Ning, Z.C. Jia, Mechanical characteristics and failure prediction of cement mortar with a sandwich structure, Minerals 9 (2019) 143.
[2] R. Jayathilakage, J. Sanjayan, P. Rajeev, Direct shear test for the assessment of rheological parameters of concrete for 3D printing applications, Mater. Struct. 52 (2019).
[3] Y. Tan, Q. Gu, J. Ning, X. Liu, Z. Jia, D. Huang, Uniaxial compression behavior of cement mortar and its damage-constitutive model based on energy theory, Materials 12 (8) (2019) 1309, https://doi.org/10.3390/ma12081309.
[4] C.-L. Khoo, Failure Criterion for Brickwork in Axial Compression PhD Thesis, University of Edinburgh, 1972.
[5] W.S. McNary, D.P. Abrams, Mechanics of masonry in compression, J. Struct. Eng. 111 (4) (1985) 857–870.
[6] R.H. Atkinson, J.L. Noland, D.P. Abrams, S. McNary, A deformation failure theory for stack-bond brick masonry prisms in compression, in: Proceedings 7th International Brick Masonry Conference, 1985, pp. 577–592.
[7] G. Mohamad, Mechanical Behavior in Failure of Concrete Block Prisms (Doctoral dissertation, Thesis (M. Sc. Degree), Federal University of Santa Catarina, Florianopolis, 1998 (in Portuguese).
[8] R. Hayen, K. Van Balen, D. Van Gemert, The mechanical behaviour of mortars in triaxial compression, in: Proceedings of Arch Bridge IV, Advances in Assessment, Structural Design and Construction, Barcelona, Spain, 2004, pp. 395–404.
[9] C.S. Barbosa, P.B. Lourenco, G. Mohamad, J.B. Hanai, Triaxial compression tests on bedding mortar samples looking at confinement effect analysis, in: North American Masonry Conference, 3–5 June, St. Louis, Missouri, USA, 2007, pp. 992–1002.
[10] G. Mohamad, F.S. Fonseca, H.R. Roman, A. Vermeltfoort, E. Rizzatti, Behavior of mortar under multiaxial stress, 12th North American Masonry Conference, 17-20 May, Denver, Colorado, 2015.
[11] Y.S. Karinski, S. Zhutovsky, V.R. Feldgun, D.Z. Yankelevsky, An experimental study on the equation of state of cementitious materials using confined compression tests, Key Eng. Mater. 711 (2016) 830–836. Trans Tech Publications.
[12] ASTM C305, Standard Practice for Mechanical Mixing of Hydraulic Cement Pastes and Mortars of Plastic Consistency, American Concrete Institutes, Detroit, USA, 2014.
[13] S. Popovics, A numerical approach to the complete stress-strain curve of concrete, Cem. Concr. Res. 3 (1973) 583–599.
[14] D.J. Carreira, K.-H. Chu, Stress-strain relationship for plain concrete in compression, ACI J. (1985) 797–804.
[15] B. De Nicolo, L. Pani, E. Pozzo, Strain of concrete at peak compressive stress for a wide range of compressive strengths, Mater. Struct. 27 (1994) 206–210.
[16] M.A. Tasdemir, C. Tasdemir, S. Akyuz, A.D. Jefferson, F.D. Lydon, B.I.J. Barr, Evaluation of strains at peak stresses in concrete: a three-phase composite model approach, Cement Concr. Compos. 20 (1998) 301–318.
[17] K. Watanabe, J. Niwa, H. Yokota, M. Iwanami, Experimental study on stress-strain curve of concrete considering localized failure in compression, J. Adv. Concr. Technol. 2 (3) (2004) 395–407.
[18] Z.-H. Lu, Y.-G. Zhao, Z.-W. Yu, Strain of high-strength concrete at peak compressive strength, Adv. Mater. Res. 446–449 (2012) 161–165.
[19] M. Attard, S. Setunge, Stress-strain relationship of confined and unconfined concrete, Mater. J. 93 (1996) 432–442.
[20] M.P. Collins, D. Mitchell, Prestressed Concrete Structures, Prentice Hall, New Jersey, 1991.
[21] E.K. Attiogbe, D. Darwin, Submicroscopic Cracking of Cement Paste and Mortar in Compression, University of Kansas, Lawrence, Kansas, USA, 1985, pp. 1–466.
[22] J.R. Sims, N.W. Krahl, S.P. Victory Jr., Triaxial Tests of Mortar and Neat Cement Cylinders, IABSE Publications, 1966.
[23] F.E. Richart, A. Brandtzaeg, R.L. Brown, A study of the failure of concrete under combined compressive stresses. Cited by GARDNER, N. J. 1969. Triaxial behaviour of concrete, ACI J. (1928) 136–146.
[24] A. Considère, Experimental Researches on Reinforced Concrete, McGraw Publishing Company, 1903.
[25] G.G. Balmer, Shearing strength of concrete under high triaxial stress-computation of Mohr's envelope as a curve, Struct Res. Lab. Rep. (1949) 23.
[26] C.V. Nielsen, Triaxial behavior of high-strength concrete and mortar, Mater. J. 95 (1998) 144–151.
[27] E. Montoya, F.J. Vecchio, S.A. Sheikh, Compression field modelling of confined concrete: constitutive models, J. Mater. Civ. Eng. 18 (2006) 510–517.
[28] W.P. Lokuge, J.G. Sanjayan, S. Setunge, Stress-strain model for laterally confined concrete, J. Mater. Civ. Eng. 17 (2005) 607–616.
[29] K.K.B. Dahl, A Constitutive Model for Normal and High Strength Concrete, Technical Institutes of Denmark, 1992.
[30] D.C. Candappa, J.G. Sanjayan, S. Setunge, Complete triaxial stress-strain curves of high-strength concrete, J. Mater. Civ. Eng. 13 (2001) 209–215.